Generalized Differential Quadrature Method for Vibration Analysis of Cantilever Trapezoidal FG Thick Plate

K. Torabi [*], H. Afshari

Department of Solid Mechanics, Faculty of Mechanical Engineering, University of Kashan, Kashan, Iran

ABSTRACT

This paper presents a numerical solution for vibration analysis of a cantilever trapezoidal thick plate. The material of the plate is considered to be graded through the thickness from a metal surface to a ceramic one according to a power law function. Kinetic and strain energies are derived based on the Reissner-Mindlin theory for thick plates and using Hamilton's principle, the governing equations and boundary conditions are derived in the Cartesian coordinates. A transformation of coordinates is used to convert the equations and boundary conditions from the original coordinate into a new computational coordinates. Generalized differential quadrature method (GDQM) is selected as a strong method and natural frequencies and corresponding modes are derived. The accuracy and convergence of the proposed solution are confirmed using results presented by other authors. Finally, the effect of the power law index, angles and thickness of the plate on the natural frequencies are investigated.

© 2016 IAU, Arak Branch.All rights reserved.

Keywords : Generalized differential quadrature method (GDQM) ; Vibration analysis; Trapezoidal plate; Functionally graded materials (FGM).

1 INTRODUCTION

TRAPEZOIDAL plates are widely used in aeronautical and civil engineering applications such as aircraft wings, ship hulls and highway bridges. The free vibration analysis of such models is a necessity to design them to operate under different loading conditions. Unlike other shapes of plate, trapezoidal thick plates have been poorly studied.

Based on the classical theory of plates, there exist a considerable amount of work related to the vibration of trapezoidal thin plates. Chopra and Durvasula [1,2] applied Galerkin's method and investigated the free vibration of simply supported symmetric and un-symmetric trapezoidal plates. Finite element method was used by Orris and Petyt [3] to study the vibration of simply supported and clamped triangular and trapezoidal plates. Using the integral equation method, the vibration analysis of cantilevered quadrilateral and trapezoidal plates was studied by Srinivasan and Babu [4]. Maruyama et al. [5] presented an experimental study of the free vibration of clamped trapezoidal plates. Bert and Malik [6] applied the differential quadrature method and presented a numerical solution for the free vibration of plates with irregular shapes. Xing and Liu [7] used differential quadrature finite element method and investigated free vibrations analysis of plates with curvilinear domain. Shufrin et al. [8] presented a semi-analytical solution for the geometrically nonlinear analysis of skew and trapezoidal plates subjected to out-of-plane loads. Using moving least square Ritz method (MLS-Ritz), Zhou and Zheng [9] presented a numerical

_____

[*]Corresponding author. Tel.: +98 36 55912448; Fax: +98 36 55559930.
E-mail address: kvntrb@kashanu.ac.ir (K. Torabi).

solution for vibration analysis of skew plates. Based on the first order shear deformation theory (FSDT), Zamani et al. [10], investigated free vibration analysis of moderately thick symmetrically laminated general trapezoidal plates with various combinations of boundary conditions.

Unlike skew and trapezoidal plates, there are considerable number of papers related to the bending, mechanical and thermal buckling and vibration analyses of homogeneous and non-homogeneous rectangular and circular thick plates, Hosseini-Hashemi et al. [11], presented an exact closed-form solution for free vibration analysis of moderately thick rectangular plates having two opposite edges simply supported. Shaban and Alipour [12], used differential transform method (DTM) and proposed a semi-analytical solution for free vibration analysis of functionally graded thick circular plates resting on the Pasternak elastic foundation with edges elastically restrained against translation and rotation. Based on the third order shear deformation plate theory and considering the in-plane displacement components of an arbitrary material point on the mid-plane of the plate, vibration analysis of a functionally graded rectangular plate resting on two parameter elastic foundation solved analytically for levy type of boundary conditions by Baferani et al. [13]. Zhu and Liew [14] employed local Kriging meshless method and studied free vibration of metal and ceramic functionally graded thick rectangular plate. Based on the 3-D elasticity theory, Hosseini-Hashemi et al. [15], presented an exact closed-form solutions for study both in-plane and out-of-plane free vibrations for thick functionally graded simply supported rectangular plates. Based on Rayleigh–Ritz procedure, Jin et al. [16] presented a new three-dimensional solution for the free vibrations of arbitrarily thick functionally graded rectangular plates with general boundary conditions.

In comparison with the thin skew and trapezoidal plates, analysis of thick ones is not considerably investigated. Xia et al. [17] hired the meshless local radial point interpolation method to study the static and free vibration analysis of a non-homogeneous moderately thick plate. Using least-square-based on finite difference method, Huang et al. [18] studied free vibration analysis of plates. An edge-based smoothed finite element method was applied for analysis of Reissner–Mindlin plates by Xuan et al. [19]. Using analytical trapezoidal p-Elements, the effect of foundation on transverse vibration of Mindlin plates was investigated by Leung and Zhu [20]. With considering corner stress singularities, Huang et al. [21] applied Ritz method and presented a solution for vibration analysis of skewed cantilevered triangular, trapezoidal and parallelogram Mindlin plates. On the basis of the CPT, FSDT and TSDT, Abrate [22] analyzed bending, buckling, and vibration of FG square, circular and skew plates with different combinations of boundary conditions. Zhao et al. [23] presented a free vibration analysis for FG square and skew plates with different boundary conditions using the element free kp-Ritz method on the basis of the FSDT. Using a simple mixed Ritz-differential quadrature (DQ) methodology, Eftekhari and Jafari [24] proposed a solution for free vibration of thick rectangular and skew plates with general boundary conditions. Petrolito [25] employed hybrid-Trefftz method and presented a numerical solution for vibration and stability analyses of thin and thick orthotropic plates.

Meanwhile, having a wide industrial applications, the cantilever plate problem is one of the most difficult boundary conditions to solve. In fact, it is because of the complexities which appear at free edges. In this paper, a numerical solution for vibration analysis of a trapezoidal Reissner-Mindlin cantilever FG plate is presented. The material of the plate is considered to vary from a metal surface to a ceramic one according to a power law function. Using Hamilton's principle, the set of governing equations and boundary conditions are derived. A transformation of coordinates is used and equations are mapped to a computational coordinates. Natural frequencies and corresponding modes are derived using differential quadrature method. The accuracy of the proposed solution is confirmed by results presented by other authors and the effect of power law index, angles and thickness of the plate on the natural frequencies are then investigated.

2 GEOMETRY OF PROBLEM
2.1 FG plate

As depicted in Fig. 1, a cantilever trapezoidal plate, clamped at x=0 is considered. The plate's material is graded through the thickness from a metal surface to a ceramic one, according to a power law function as the following relations:

$$E(z) = E_m + (E_c - E_m)\left(\frac{1}{2} + \frac{z}{h}\right)^q \quad , \quad \rho(z) = \rho_m + (\rho_c - \rho_m)\left(\frac{1}{2} + \frac{z}{h}\right)^q \tag{1}$$

where q is the power law index, h is thickness of the plate and E and ρ are modulus of elasticity and density of the materials, respectively. Meanwhile, subscripts "c" and "m" are used to indicate corresponding properties in ceramic and metal, respectively. It should be noted that Poisson's ratio (v) is considered to be constant through the thickness.

Eq. (1) can be rewritten in a dimensionless form as:

$$\frac{E}{E_m} = 1 + \left(\frac{\mu_E - 1}{2^q}\right)(1+\xi)^q \quad , \quad \frac{\rho}{\rho_m} = 1 + \left(\frac{\mu_\rho - 1}{2^q}\right)(1+\xi)^q \tag{2}$$

where

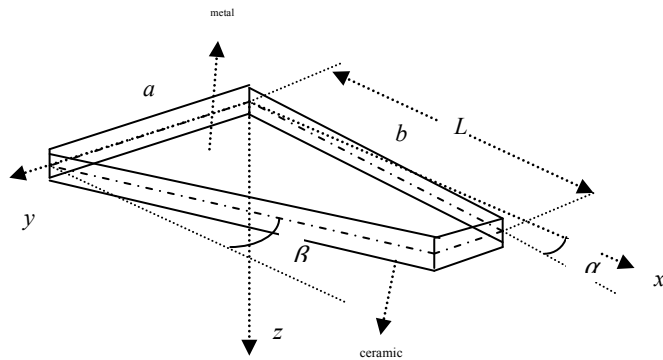$$\xi = 2z/h \qquad \mu_E = E_c/E_m \qquad \mu_\rho = \rho_c/\rho_m \tag{3}$$

Fig.1
Geometry of the trapezoidal thick plate.

2.2 Reissner-Mindlin theory of plates

According to the Reissner-Mindlin theory, in which the in-plane displacements are considered as linear functions of the plate thickness and the transverse deflection is considered to be constant through the plate thickness, the displacement field is used as follows [26]:

$$\begin{aligned}
u^z(x,y,z) &= u(x,y) + z\,\psi_x(x,y) \\
v^z(x,y,z) &= v(x,y) + z\,\psi_y(x,y) \\
w^z(x,y,z) &= w(x,y)
\end{aligned} \tag{4}$$

where u^z, v^z and w^z show the components of displacement along x, y and z directions, respectively; u, v and w indicate components of displacement on the middle surface ($z=0$) along x, y and z directions, respectively. Also ψ_x and ψ_y are rotations about y and x axes, respectively. The notation that ψ_x represents the rotation about the y-axis and vice versa may be confusing and in addition they do not follow the right-hand rule. However, these notations will be used herein because of their extensive use in the open literature [27].

By neglecting in-plane deformations of plate at the middle surface, Eq. (4) can be summarized as:

$$\begin{aligned}
u^z(x,y,z) &= z\,\psi_x(x,y) \\
v^z(x,y,z) &= z\,\psi_y(x,y) \\
w^z(x,y,z) &= w(x,y)
\end{aligned} \tag{5}$$

Now, according to strain-displacement equations, components of strain of the plate can be stated as:

$$\varepsilon_x = \frac{\partial u^z}{\partial x} = z\frac{\partial \psi_x}{\partial x} \quad , \quad \varepsilon_y = \frac{\partial v^z}{\partial y} = z\frac{\partial \psi_y}{\partial y} \quad , \quad \varepsilon_z = \frac{\partial w^z}{\partial z} \approx 0$$

$$\gamma_{xy} = \frac{\partial u^z}{\partial y} + \frac{\partial v^z}{\partial x} = z\left(\frac{\partial \psi_x}{\partial y} + \frac{\partial \psi_y}{\partial x}\right) \quad , \quad \gamma_{xz} = \frac{\partial u^z}{\partial z} + \frac{\partial w^z}{\partial x} = \psi_x + \frac{\partial w}{\partial x} \quad , \tag{6}$$

$$\gamma_{yz} = \frac{\partial v^z}{\partial z} + \frac{\partial w^z}{\partial y} = \psi_y + \frac{\partial w}{\partial y}$$

It should be pointed out that the normal transverse stress is assumed to be zero.

By neglecting σ_z in comparison with σ_x and σ_y, using Hook's laws, components of stress of the plate can be obtained as:

$$\sigma_x = \frac{E}{1-v^2}(\varepsilon_x + v\,\varepsilon_y) = \frac{E}{1-v^2}\left(\frac{\partial \psi_x}{\partial x} + v\frac{\partial \psi_y}{\partial y}\right)$$

$$\sigma_y = \frac{E}{1-v^2}(\varepsilon_y + v\,\varepsilon_x) = \frac{E}{1-v^2}\left(\frac{\partial \psi_y}{\partial y} + v\frac{\partial \psi_x}{\partial x}\right) \qquad \sigma_z = 0 \tag{7}$$

$$\sigma_{xy} = G\gamma_{xy} = Gz\left(\frac{\partial \psi_x}{\partial y} + \frac{\partial \psi_y}{\partial x}\right) \quad , \quad \sigma_{xz} = kG\gamma_{xz} = kG\left(\psi_x + \frac{\partial w}{\partial x}\right)$$

$$\sigma_{yz} = kG\gamma_{yz} = kG\left(\psi_y + \frac{\partial w}{\partial y}\right)$$

In which G is shear modulus and k is "shear correction factor" introduced to make up the geometry-dependent distribution of shear stress. This factor depends on the shape of the section and Poisson's ratio of material, in this paper following relation is used [28]:

$$k = (5+5v)/(6+5v) \tag{8}$$

2.3 Hamilton's principle

Hamilton's principle states that of all the paths of admissible configurations that the body can take as it moves from configuration "1" at time t_1 to configuration "2" at time t_2, the path that satisfies Newton's second law at each instant during the interval is the path that extremizes the time integral of the Lagrangian ($L=U-T$) during the interval; this principle can be stated in the mathematical form as:

$$\delta\int_{t_1}^{t_2}(U-T)dt = 0 \tag{9}$$

where U and T are strain and kinetic forms of energy, respectively; The kinetic energy of the plate can be considered as:

$$T = \frac{1}{2}\iiint_V \rho(z)\left[\left(\frac{\partial u^z}{\partial t}\right)^2 + \left(\frac{\partial v^z}{\partial t}\right)^2 + \left(\frac{\partial w^z}{\partial t}\right)^2\right]dV \tag{10}$$

and strain energy can be stated as:

$$U = \iiint_V (\sigma_x\varepsilon_x + \sigma_y\varepsilon_y + \sigma_z\varepsilon_z + \sigma_{xy}\gamma_{xy} + \sigma_{yz}\gamma_{yz} + \sigma_{yz}\gamma_{yz})dV \tag{11}$$

Substituting Eqs. (6), (7), (10) and (11) into the Eq. (9), leads to

$$\delta w : \frac{\partial Q_x}{\partial x} + \frac{\partial Q_y}{\partial y} = I_0 \frac{\partial^2 w}{\partial t^2} \tag{12a}$$

$$\delta \psi_x : \frac{\partial M_x}{\partial x} + \frac{\partial M_y}{\partial y} - Q_x = I_2 \frac{\partial^2 \psi_x}{\partial t^2} \tag{12b}$$

$$\delta \psi_y : \frac{\partial M_y}{\partial y} + \frac{\partial M_{xy}}{\partial x} - Q_y = I_2 \frac{\partial^2 \psi_y}{\partial t^2} \tag{12c}$$

$$\int_{t_1}^{t_2} \oiint_\Gamma \left(M_x \delta\psi_x dy - M_y \delta\psi_y dx + M_{xy} \delta\psi_y dy - M_{xy} \delta\psi_x dx + Q_x \delta w dy - Q_y \delta w dx \right) dt = 0 \tag{12d}$$

where Γ is boundary path and stress resultants are defined as follows:

$$\begin{Bmatrix} M_x \\ M_y \\ M_{xy} \end{Bmatrix} = \int_{-\frac{h}{2}}^{\frac{h}{2}} \begin{Bmatrix} \sigma_x \\ \sigma_y \\ \sigma_{xy} \end{Bmatrix} z dz = D \begin{Bmatrix} \frac{\partial \psi_x}{\partial x} + v \frac{\partial \psi_y}{\partial y} \\ \frac{\partial \psi_y}{\partial y} + v \frac{\partial \psi_x}{\partial x} \\ \frac{1-v}{2} \left(\frac{\partial \psi_x}{\partial y} + \frac{\partial \psi_y}{\partial x} \right) \end{Bmatrix} \quad , \quad \begin{Bmatrix} Q_x \\ Q_y \end{Bmatrix} = \int_{-\frac{h}{2}}^{\frac{h}{2}} \begin{Bmatrix} \sigma_{xz} \\ \sigma_{yz} \end{Bmatrix} dz = \frac{1-v}{2} kA \begin{Bmatrix} \psi_x + \frac{\partial w}{\partial x} \\ \psi_y + \frac{\partial w}{\partial y} \end{Bmatrix} \tag{13}$$

In which

$$\begin{Bmatrix} A \\ D \end{Bmatrix} = \int_{-\frac{h}{2}}^{\frac{h}{2}} \frac{E(z)}{1-v^2} \begin{Bmatrix} 1 \\ z^2 \end{Bmatrix} dz \tag{14}$$

and translational and rotational inertias of the plate are defined as:

$$\begin{Bmatrix} I_0 \\ I_2 \end{Bmatrix} = \int_{-\frac{h}{2}}^{\frac{h}{2}} \rho(z) \begin{Bmatrix} 1 \\ z^2 \end{Bmatrix} dz \tag{15}$$

Substituting Eq. (13) into the Eqs. (12a)-(12c), the set of governing equations can be stated as:

$$v_1 kA \left(\frac{\partial^2 w}{\partial x^2} + \frac{\partial^2 w}{\partial y^2} + \frac{\partial \psi_x}{\partial x} + \frac{\partial \psi_y}{\partial y} \right) = I_0 \frac{\partial^2 w}{\partial t^2} \tag{16a}$$

$$D \left(\frac{\partial^2 \psi_x}{\partial x^2} + v_1 \frac{\partial^2 \psi_x}{\partial y^2} + v_2 \frac{\partial^2 \psi_y}{\partial x \partial y} \right) - v_1 kA \left(\psi_x + \frac{\partial w}{\partial x} \right) = I_2 \frac{\partial^2 \psi_x}{\partial t^2} \tag{16b}$$

$$D \left(\frac{\partial^2 \psi_y}{\partial y^2} + v_1 \frac{\partial^2 \psi_y}{\partial x^2} + v_2 \frac{\partial^2 \psi_x}{\partial x \partial y} \right) - v_1 kA \left(\psi_y + \frac{\partial w}{\partial y} \right) = I_2 \frac{\partial^2 \psi_y}{\partial t^2} \tag{16c}$$

where

$$v_1 = (1-v)/2 \qquad v_2 = (1+v)/2 \tag{17}$$

Also, using Eqs. (1) and (2), Eqs. (14) and (15) can be rewritten in the following dimensionless form:

$$\begin{Bmatrix} A \\ D \end{Bmatrix} = \begin{Bmatrix} A_m f_0 \\ D_m f_2 \end{Bmatrix} \quad , \quad \begin{Bmatrix} I_0 \\ I_2 \end{Bmatrix} = \rho_m \begin{Bmatrix} g_0 h \\ g_2 h^3/12 \end{Bmatrix} \tag{18}$$

In which

$$A_m = \frac{E_m h}{1-v^2} \qquad D_m = \frac{E_m h^3}{12(1-v^2)}$$

$$f_0 = 1 + \frac{\mu_E - 1}{q+1} \qquad f_2 = 1 + \frac{3(\mu_E - 1)(q^2 + q + 2)}{(q+1)(q+2)(q+3)} \qquad g_0 = 1 + \frac{\mu_q - 1}{q+1} \qquad g_2 = 1 + \frac{3(\mu_q - 1)(q^2 + q + 2)}{(q+1)(q+2)(q+3)} \tag{19}$$

Considering a portion of the path Γ, the rectangular coordinates *x-y* are related to the normal and tangential coordinates *n-s* by

$$dx = -ds \sin\theta \qquad dy = ds \cos\theta \tag{20}$$

The bending rotations can be expressed in terms of their normal-tangential components by

$$\psi_x = \psi_n \cos\theta - \psi_s \sin\theta \qquad \psi_y = \psi_n \sin\theta + \psi_s \cos\theta \tag{21}$$

where the subscripts "*n*" and "*s*" show the normal and tangential directions, respectively. Substituting Eqs. (20) and (21) into the Eq. (12d), boundary conditions can be stated as:

$$\begin{aligned} \delta w &: Q_n = 0 \quad or \quad w = 0 \\ \delta\psi_n &: M_{nn} = 0 \quad or \quad \psi_n = 0 \\ \delta\psi_s &: M_{ns} = 0 \quad or \quad \psi_s = 0 \end{aligned} \tag{22}$$

where M_{nn}, M_{nn}, M_{ns} and Q_n are the bending moment normal to the edge, the twisting moment at the edge and the shear force, respectively. These parameters are defined as:

$$\begin{aligned} M_{nn} &= M_x \cos^2\theta + M_y \sin^2\theta + M_{xy} \sin 2\theta \\ M_{ns} &= \left(\frac{M_y - M_x}{2} \right) \sin 2\theta + M_{xy} \cos 2\theta \\ Q_n &= Q_x \cos\theta + Q_y \sin\theta \end{aligned} \tag{23}$$

2.4 Geometry mapping

The analysis of the nonrectangular plates uses a local parameter coordinate system rather than a Cartesian one. As Fig. 2 shows, the original trapezoidal shape of the plate in the *x–y* coordinate system is mapped to a square in the $\zeta - \eta$ coordinates, using the following transformation:

$$W^*(x + iy) = \zeta + i\eta \tag{24}$$

In which

$$x = a\zeta + L\eta(\tan\alpha - G\zeta) \qquad y = L\eta \qquad G = \tan\alpha - \tan\beta \tag{25}$$

Inverse form of Eq. (25) can be rewritten as:

$$\zeta = \frac{x - y\tan\alpha}{a - Gy} \qquad\qquad \eta = y/L \tag{26}$$

which leads to the following relations for derivatives:

$$
\frac{\partial}{\partial x} = \frac{E(\eta)}{L}\frac{\partial}{\partial\zeta} \qquad\qquad \frac{\partial}{\partial y} = \frac{1}{L}\left[\frac{\partial}{\partial\eta} + F(\zeta)E(\eta)\frac{\partial}{\partial\zeta}\right] \qquad\qquad \frac{\partial^2}{\partial x^2} = \frac{E^2(\eta)}{L^2}\frac{\partial^2}{\partial\zeta^2}
$$

$$
\frac{\partial^2}{\partial y^2} = \frac{1}{L^2}\left[\frac{\partial^2}{\partial\eta^2} + F^2(\zeta)E^2(\eta)\frac{\partial^2}{\partial\zeta^2} + 2F(\zeta)E(\eta)\frac{\partial^2}{\partial\zeta\partial\eta} + 2GF(\zeta)E^2(\eta)\frac{\partial}{\partial\zeta}\right] \tag{27}
$$

$$
\frac{\partial^2}{\partial x\partial y} = \frac{1}{L^2}\left[E(\eta)\frac{\partial}{\partial\zeta\partial\eta} + F(\zeta)E^2(\eta)\frac{\partial^2}{\partial\zeta^2} + GE^2(\eta)\frac{\partial}{\partial\zeta}\right]
$$

where

$$E(\eta) = \frac{L}{a - GL\eta} = \frac{\cos\alpha}{\varphi - G\eta\cos\alpha} \qquad\qquad F(\zeta) = G\zeta - \tan\alpha \qquad\qquad \varphi = a/b \tag{28}$$

Note that in deriving Eq. (27), following relation is used:

$$\frac{dE(\eta)}{d\eta} = GE^2(\eta) \tag{29}$$

Using Eq. (27), the set of governing Eqs. (16a)-(16c) can be stated as:

$$
\left[1 + F^2(\zeta)\right]E^2(\eta)\frac{\partial^2\bar{w}}{\partial\zeta^2} + \frac{\partial^2\bar{w}}{\partial\eta^2} + 2F(\zeta)E(\eta)\frac{\partial^2\bar{w}}{\partial\zeta\partial\eta} + 2GF(\zeta)E^2(\eta)\frac{\partial\bar{w}}{\partial\zeta}
$$

$$
+ E(\eta)\cos\alpha\frac{\partial\psi_x}{\partial\zeta} + \cos\alpha\frac{\partial\psi_y}{\partial\eta} + F(\zeta)E(\eta)\cos\alpha\frac{\partial\psi_y}{\partial\zeta} = \frac{I_0 b^2\cos^2\alpha}{v_1 kA}\frac{\partial^2\bar{w}}{\partial t^2} \tag{30a}
$$

$$
\left[1 + v_1 F^2(\zeta)\right]E^2(\eta)\frac{\partial^2\psi_x}{\partial\zeta^2} + v_1\frac{\partial^2\psi_x}{\partial\eta^2} + 2v_1 F(\zeta)E(\eta)\frac{\partial^2\psi_x}{\partial\zeta\partial\eta} + 2v_1 GF(\zeta)E^2(\eta)\frac{\partial\psi_x}{\partial\zeta}
$$

$$
+ v_2 F(\zeta)E^2(\eta)\frac{\partial^2\psi_y}{\partial\zeta^2} + v_2 E(\eta)\frac{\partial\psi_y}{\partial\zeta\partial\eta} + v_2 GE^2(\eta)\frac{\partial\psi_y}{\partial\zeta}
$$

$$
- \frac{v_1 kAb^2}{D}\left(\cos^2\alpha\psi_x + E(\eta)\cos\alpha\frac{\partial\bar{w}}{\partial\zeta}\right) = \frac{I_2 b^2\cos^2\alpha}{D}\frac{\partial^2\psi_x}{\partial t^2} \tag{30b}
$$

$$
\frac{\partial^2\psi_y}{\partial\eta^2} + \left[F(\zeta) + v_1\right]E^2(\eta)\frac{\partial^2\psi_y}{\partial\zeta^2} + 2F(\zeta)E\frac{\partial^2\psi_y}{\partial\zeta\partial\eta} + 2GF(\zeta)E^2(\eta)\frac{\partial\psi_y}{\partial\zeta}
$$

$$
+ v_2 F(\zeta)E^2(\eta)\frac{\partial^2\psi_x}{\partial\zeta^2} + v_2 E(\eta)\frac{\partial\psi_x}{\partial\zeta\partial\eta} + v_2 GE^2(\eta)\frac{\partial\psi_x}{\partial\zeta}
$$

$$
- \frac{v_1 kAb^2}{D}\left(\cos^2\alpha\psi_y + \cos\alpha\frac{\partial\bar{w}}{\partial\eta} + \cos\alpha F(\zeta)E(\eta)\frac{\partial\bar{w}}{\partial\zeta}\right) = \frac{I_2 b^2\cos^2\alpha}{D}\frac{\partial^2\psi_y}{\partial t^2} \tag{30c}
$$

where

$$\bar{w} = w/b \tag{31}$$

Using the method of separation of variables as:

$$\begin{aligned}
\bar{w}(\zeta,\eta,t) &= W(\zeta,\eta)\exp(i\omega t) \\
\psi_x(\zeta,\eta,t) &= \Psi_x(\zeta,\eta)\exp(i\omega t) \\
\psi_y(\zeta,\eta,t) &= \Psi_y(\zeta,\eta)\exp(i\omega t)
\end{aligned} \tag{32}$$

The set of Eqs. (30a)-(30c) can be rewritten as:

$$\begin{aligned}
&\left[1+F^2(\zeta)\right]E^2(\eta)\frac{\partial^2 W}{\partial\zeta^2} + \frac{\partial^2 W}{\partial\eta^2} + 2F(\zeta)E(\eta)\frac{\partial^2 W}{\partial\zeta\partial\eta} + 2GF(\zeta)E^2(\eta)\frac{\partial W}{\partial\zeta} \\
&+E(\eta)\cos\alpha\frac{\partial\Psi_x}{\partial\zeta} + \cos\alpha\frac{\partial\psi_y}{\partial\eta} + F(\zeta)E(\eta)\cos\alpha\frac{\partial\Psi_y}{\partial\zeta} + \frac{1}{v_1 k}\frac{\gamma^2\cos^2\alpha}{12}\frac{g_0}{f_0}\lambda^2 W = 0
\end{aligned} \tag{33a}$$

$$\begin{aligned}
&\left[1+v_1 F^2(\zeta)\right]E^2(\eta)\frac{\partial^2\Psi_x}{\partial\zeta^2} + v_1\frac{\partial^2\Psi_x}{\partial\eta^2} + 2v_1 F(\zeta)E(\eta)\frac{\partial^2\Psi_x}{\partial\zeta\partial\eta} + 2v_1 GF(\zeta)E^2(\eta)\frac{\partial\Psi_x}{\partial\zeta} \\
&+v_2 F(\zeta)E^2(\eta)\frac{\partial^2\Psi_y}{\partial\zeta^2} + v_2 E(\eta)\frac{\partial\psi_y}{\partial\zeta\partial\eta} + v_2 GE^2(\eta)\frac{\partial\Psi_y}{\partial\zeta} \\
&-\frac{12v_1 k}{\gamma^2}\frac{f_0}{f_2}\left(\cos^2\alpha\Psi_x + E(\eta)\cos\alpha\frac{\partial W}{\partial\zeta}\right) + \frac{\gamma^2\cos^2\alpha}{12}\frac{g_2}{f_2}\lambda^2\Psi_x = 0
\end{aligned} \tag{33b}$$

$$\begin{aligned}
&\frac{\partial^2\Psi_y}{\partial\eta^2} + \left[F^2(\zeta)+v_1\right]E^2(\eta)\frac{\partial^2\Psi_y}{\partial\zeta^2} + 2F(\zeta)E(\eta)\frac{\partial^2\Psi_y}{\partial\zeta\partial\eta} + 2GF(\zeta)E^2(\eta)\frac{\partial\Psi_y}{\partial\zeta} \\
&+v_2 F(\zeta)E^2(\eta)\frac{\partial\Psi_x}{\partial\zeta^2} + v_2 E(\eta)\frac{\partial\Psi_x}{\partial\zeta\partial\eta} + v_2 GE^2(\eta)\frac{\partial\Psi_y}{\partial\zeta} \\
&-\frac{12v_1 k}{\gamma^2}\frac{f_0}{f_2}\left(\cos^2\alpha\Psi_y + \cos\alpha\frac{\partial W}{\partial\eta} + \cos\alpha F(\zeta)E(\eta)\frac{\partial W}{\partial\zeta}\right) + \frac{\gamma^2\cos^2\alpha}{12}\frac{g_2}{f_2}\lambda^2\Psi_y = 0
\end{aligned} \tag{33c}$$

In which

$$\lambda^2 = \frac{\rho_m h b^4 \omega^2}{D_m} \qquad \gamma = h/b \tag{34}$$

Also dimensionless form of the boundary conditions can be derived using Eqs. (13), (22)-(24) and (27) as:

$$\eta = 0 \qquad \Psi_x = 0 \qquad \Psi_y = 0 \qquad W = 0 \tag{35a}$$

$$\begin{aligned}
&\eta = 1 \quad \left(\theta = \frac{\pi}{2}\right) \\
&M_{nn} = \frac{D}{L}\left[\frac{\partial\Psi_y}{\partial\eta} + \frac{F(\zeta)\cos\alpha}{\varphi - G\cos\alpha}\frac{\partial\Psi_y}{\partial\zeta} + \frac{v\cos\alpha}{\varphi - G\cos\alpha}\frac{\partial\Psi_x}{\partial\zeta}\right] = 0 \\
&M_{ns} = -\frac{Dv_1}{L}\left[\frac{\partial\Psi_x}{\partial\eta} + \frac{F(\zeta)\cos\alpha}{\varphi - G\cos\alpha}\frac{\partial\Psi_x}{\partial\zeta} + \frac{\cos\alpha}{\varphi - G\cos\alpha}\frac{\partial\Psi_y}{\partial\zeta}\right] = 0 \\
&Q_n = v_1 kA\left[\Psi_y + \sec\alpha\frac{\partial W}{\partial\eta} + \frac{F(\zeta)}{\varphi - G\cos\alpha}\frac{\partial W}{\partial\zeta}\right] = 0
\end{aligned} \tag{35b}$$

$\zeta = 0 \quad (\theta = \pi - \alpha)$

$$M_{nn} = \frac{D}{L} \left\{ \begin{array}{l} E(\eta)\dfrac{\partial \Psi_x}{\partial \zeta} + v\dfrac{\partial \Psi_y}{\partial \eta} - v\tan\alpha E(\eta)\dfrac{\partial \Psi_y}{\partial \zeta}\cos^2\alpha \\ + \dfrac{\partial \Psi_y}{\partial \eta} - \tan\alpha E(\eta)\dfrac{\partial \Psi_y}{\partial \zeta} + vE(\eta)\dfrac{\partial \Psi_x}{\partial \zeta}\sin^2\alpha \\ -v_1\left[\dfrac{\partial \Psi_x}{\partial \eta} - \tan\alpha E(\eta)\dfrac{\partial \Psi_x}{\partial \zeta} + E(\eta)\dfrac{\partial \Psi_y}{\partial \zeta}\sin 2\alpha\right] \end{array} \right\}$$

$$M_{ns} = \frac{Dv_1}{L}\left\{ \begin{array}{l} \left[E(\eta)\dfrac{\partial \Psi_x}{\partial \zeta} - \dfrac{\partial \Psi_y}{\partial \eta} + \tan\alpha E(\eta)\dfrac{\partial \Psi_y}{\partial \zeta}\sin 2\alpha\right] \\ + \left[\dfrac{\partial \Psi_x}{\partial \eta} - \tan\alpha E(\eta)\dfrac{\partial \Psi_x}{\partial \zeta} + E(\eta)\dfrac{\partial \Psi_y}{\partial \zeta}\cos 2\alpha\right] \end{array} \right\}$$

$$Q_n = v_1 kA\left\{ \left[\Psi_y + \sec\alpha\dfrac{\partial W}{\partial \eta} - \dfrac{\tan\alpha E(\eta)}{\cos\alpha}\dfrac{\partial W}{\partial \zeta}\right]\sin\alpha - \left[\Psi_x + \dfrac{E(\eta)}{\cos\alpha}\dfrac{\partial W}{\partial \zeta}\cos\alpha\right] \right\} = 0$$

(35c)

$\zeta = 1 \quad (\theta = -\beta)$

$$M_{nn} = \frac{D}{L}\left\{ \begin{array}{l} \left[E(\eta)\dfrac{\partial \Psi_x}{\partial \zeta} + v\dfrac{\partial \Psi_y}{\partial \eta} - v\tan\beta E(\eta)\dfrac{\partial \Psi_y}{\partial \zeta}\right]\cos^2\beta \\ + \left[\dfrac{\partial \Psi_y}{\partial \eta} - \tan\beta E(\eta)\dfrac{\partial \Psi_y}{\partial \zeta} + vE(\eta)\dfrac{\partial \Psi_x}{\partial \zeta}\right]\sin^2\beta \\ -v_1\left[\dfrac{\partial \Psi_x}{\partial \eta} - \tan\beta E(\eta)\dfrac{\partial \Psi_x}{\partial \zeta} + E(\eta)\dfrac{\partial \Psi_y}{\partial \zeta}\sin 2\beta\right] \end{array} \right\}$$

$$M_{ns} = \frac{Dv_1}{L}\left\{ \begin{array}{l} \left[E(\eta)\dfrac{\partial \Psi_x}{\partial \zeta} - \dfrac{\partial \Psi_y}{\partial \eta} + \tan\beta E(\eta)\dfrac{\partial \Psi_y}{\partial \zeta}\sin 2\beta\right] \\ + \left[\dfrac{\partial \Psi_x}{\partial \eta} - \tan\beta E(\eta)\dfrac{\partial \Psi_x}{\partial \zeta} + E(\eta)\dfrac{\partial \Psi_y}{\partial \zeta}\cos 2\beta\right] \end{array} \right\}$$

$$Q_n = v_1 kA\left\{ \left[\Psi_x + \dfrac{E(\eta)}{\cos\alpha}\dfrac{\partial W}{\partial \zeta}\right]\cos\beta - \left[\Psi_y + \sec\alpha\dfrac{\partial W}{\partial \eta} - \dfrac{\tan\beta E(\eta)}{\cos\alpha}\dfrac{\partial W}{\partial \zeta}\right]\sin\beta \right\} = 0$$

(35d)

It should be noted that in deriving Eqs. (35a)-(35d), following relations are used:

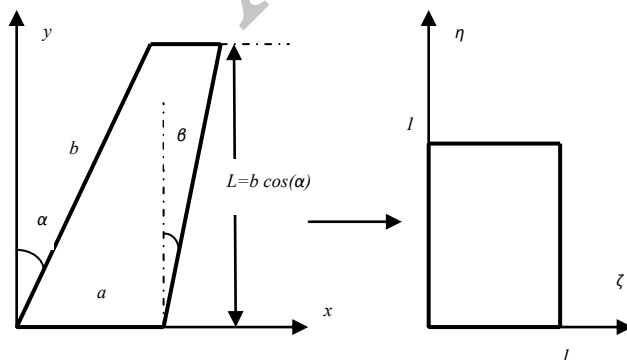$$F(0) = -\tan\alpha \qquad F(1) = -\tan\beta \qquad E(1) = \frac{\cos\alpha}{\varphi - G\cos\alpha} \tag{36}$$

Fig.2
Original and computational coordinates.

3   DIFFERNTIAL QUADRATURE METHOD (DQM)

Consider $f(\zeta, \eta)$ as a two dimensional function. Values of this function at $N*M$ pre-selected grid of points can be considered as:

$$f_{ij} = f(\zeta_i, \eta_j) \qquad i = 1, 2, ..., N \qquad j = 1, 2, ..., M \tag{37}$$

The differential quadrature method is based on the idea that all derivatives of a function can be easily approximated by means of weighted linear sum of the function values at the pre-selected grid of points as:

$$\frac{\partial f}{\partial \zeta}\Big|_{(\zeta,\eta)=(\zeta_i \eta_j)} = \sum_{n=1}^{N} A_{in}^{(\zeta)} f_{nj} \qquad \frac{\partial^2 f}{\partial \zeta^2}\Big|_{(\zeta,\eta)=(\zeta_i \eta_j)} = \sum_{n=1}^{N} B_{in}^{(\zeta)} f_{nj} \qquad \frac{\partial f}{\partial \eta}\Big|_{(\zeta,\eta)=(\zeta_i \eta_j)} = \sum_{m=1}^{M} A_{jm}^{(\eta)} f_{im}$$

$$\frac{\partial^2 f}{\partial \eta^2}\Big|_{(\zeta,\eta)=(\zeta_i \eta_j)} = \sum_{m=1}^{M} B_{jm}^{(\eta)} f_{im} \qquad \frac{\partial^2 f}{\partial \zeta \partial \eta}\Big|_{(\zeta,\Theta)=(\zeta_i \eta_j)} = \sum_{n=1}^{N} A_{jm}^{(\zeta)} f_{nm} \tag{38}$$

where $A^{(\zeta)}, B^{(\zeta)}, A^{(\eta)}$ and $B^{(\eta)}$ are the weighting coefficients associated with the first and second order derivatives in ζ and η directions, respectively. These matrices for the first-order derivatives are given by [29]

$$A_{in}^{(\zeta)} = \begin{cases} \dfrac{\prod\limits_{\substack{k=1 \\ k \neq i,n}}^{N} (\zeta_i - \zeta_k)}{\prod\limits_{\substack{k=1 \\ k \neq n}}^{N} (\zeta_n - \zeta_k)}, (i, n = 1, 2, 3, ..., N; i \neq n) \\[3em] \sum\limits_{\substack{k=1 \\ k \neq i}}^{N} \dfrac{1}{(\zeta_i - \zeta_k)}, (i = n = 1, 2, 3, ..., N) \end{cases}$$

$$A_{jm}^{(\eta)} = \begin{cases} \dfrac{\prod\limits_{\substack{k=1 \\ k \neq j,m}}^{M} (\eta_j - \eta_k)}{\prod\limits_{\substack{k=1 \\ k \neq m}}^{M} (\eta_m - \eta_k)}, (j, m = 1, 2, 3, ..., M; j \neq m) \\[3em] \sum\limits_{\substack{k=1 \\ k \neq j}}^{M} \dfrac{1}{(\eta_j - \eta_k)}, (j = m = 1, 2, 3, ..., M) \end{cases} \tag{39}$$

and of second-order derivatives are extracted from the following relations:

$$B^{(\zeta)} = A^{(\zeta)} A^{(\zeta)} \qquad B^{(\eta)} = A^{(\eta)} A^{(\eta)} \tag{40}$$

A convenient option for the grid points are the equally spaced points. Another choice which gives more accurate results is unequally spaced grid points [29]. A well-accepted set of the grid points is the Gauss–Lobatto–Chebyshev points given for interval [0,1] by

$$\zeta_i = \frac{1}{2}\left\{1 - \cos\left[\frac{(i-1)\pi}{(N-1)}\right]\right\} \qquad \eta_j = \frac{1}{2}\left\{1 - \cos\left[\frac{(j-1)\pi}{(M-1)}\right]\right\} \tag{41}$$

4   DQ ANALOGUE

Using DQ rules, the set of governing differential Eqs. (33a)-(33c) is transformed to the following form:

$$
\begin{aligned}
&\left[1+F^2(\zeta_i)\right]E^2(\eta_j)\sum_{n=1}^{N}B_{in}^{(\zeta)}W_{nj}+\sum_{n=1}^{N}B_{jm}^{(\eta)}W_{im}+2F(\zeta_i)E(\eta_j)\sum_{n=1}^{N}A_{in}^{(\zeta)}\sum_{m=1}^{M}A_{jm}^{(\eta)}W_{nm}\\
&+2GF(\zeta_i)E^2(\eta_j)\sum_{n=1}^{N}A_{in}^{(\zeta)}W_{nj}+E(\eta_j)\cos\alpha\sum_{n=1}^{N}A_{in}^{(\zeta)}\Phi_{nj}+\cos\alpha\sum_{n=1}^{N}A_{jm}^{(\eta)}\Theta_{im}\\
&+F(\zeta_i)E(\eta_j)\cos\alpha\sum_{n=1}^{N}A_{in}^{(\zeta)}\Theta_{nj}+\frac{1}{v_1k}\frac{\gamma^2\cos^2\alpha}{12}\frac{g_0}{f_0}\lambda^2W_{ij}=0
\end{aligned}
\tag{42a}
$$

$$
\begin{aligned}
&\left[1+v_1F^2(\zeta_i)\right]E^2(\eta_j)\sum_{n=1}^{N}B_{in}^{(\zeta)}\Phi_{nj}+v_1\sum_{m=1}^{M}B_{jm}^{(\eta)}\Phi_{im}+2v_1F(\zeta_i)E(\eta_j)\sum_{n=1}^{N}A_{in}^{(\zeta)}\sum_{m=1}^{M}A_{jm}^{(\eta)}\Phi_{nm}\\
&+2v_1GF(\zeta_i)E^2(\eta_j)\sum_{n=1}^{N}A_{in}^{(\zeta)}\Phi_{nj}+v_2F(\zeta_i)E^2(\eta_j)\sum_{n=1}^{N}B_{in}^{(\zeta)}\Theta_{nj}+v_2E(\eta_j)\sum_{n=1}^{N}A_{in}^{(\zeta)}\sum_{m=1}^{M}A_{jm}^{(\eta)}\Theta_{nm}\\
&+v_2GE^2(\eta_j)\sum_{n=1}^{N}A_{in}^{(\zeta)}\Theta_{nj}-12v_1\frac{k}{\gamma^2}\frac{f_0}{f_2}\left(\cos^2\alpha\Phi_{ij}+E(\eta_j)\cos\alpha\sum_{n=1}^{N}A_{in}^{(\zeta)}W_{nj}\right)+\frac{\gamma^2\cos^2\alpha k}{12}\frac{g_2}{f_2}\lambda^2\Phi_{ij}=0
\end{aligned}
\tag{42b}
$$

$$
\begin{aligned}
&\sum_{m=1}^{M}B_{jm}^{(\eta)}\Theta_{im}+\left[F^2(\zeta_i)+v_1\right]E^2(\eta_j)\sum_{n=1}^{N}B_{in}^{(\zeta)}\Theta_{nj}+2F(\zeta_i)E(\eta_j)\sum_{n=1}^{N}A_{in}^{(\zeta)}\sum_{m=1}^{M}A_{jm}^{(\eta)}\Theta_{nm}\\
&+2GF(\zeta_i)E^2(\eta_j)\sum_{n=1}^{N}A_{in}^{(\zeta)}\Theta_{nj}+v_2F(\zeta_i)E^2(\eta_j)\sum_{n=1}^{N}B_{in}^{(\zeta)}\Phi_{nj}+v_2E(\eta_j)\sum_{n=1}^{N}A_{in}^{(\zeta)}\sum_{m=1}^{M}A_{jm}^{(\eta)}\Phi_{nm}\\
&+v_2GE^2(\eta_j)\sum_{n=1}^{N}A_{in}^{(\zeta)}\Phi_{nj}-12v_1\frac{k}{\gamma^2}\frac{f_0}{f_2}\left(\cos^2\alpha\Theta_{ij}+\cos\alpha\sum_{m=1}^{M}A_{jm}^{(\eta)}W_{im}+F(\zeta_i)E(\eta_j)\cos\alpha\sum_{n=1}^{N}A_{in}^{(\zeta)}W_{nj}\right)\\
&+\frac{\gamma^2\cos^2\alpha}{12}\frac{g_2}{f_2}\lambda^2\Theta_{ij}=0
\end{aligned}
\tag{42c}
$$

where

$$
W_{ij}=W(\zeta_i,\eta_j)\qquad,\Phi_{ij}=\Psi_x(\zeta_i,\eta_j)\qquad,\Theta_{ij}=\Psi_y(\zeta_i,\eta_j)
\tag{43}
$$

Using following defined vectors:

$$
\hat{W}=W_{ij}\qquad,\hat{\Phi}_v=\Phi_{ij}\qquad,\hat{\Theta}_v=\Theta_{ij}\qquad,v=(j-1)N+i
\tag{44}
$$

Eqs. (42a)-(42c) can be rewritten as:

$$
[P_W]\{\hat{W}\}+[P_\Phi]\{\hat{\Phi}\}+[P_\Theta]\{\hat{\Theta}\}+\frac{1}{kv_1}\frac{\gamma^2\cos^2\alpha}{12}\frac{g_0}{f_0}\lambda^2\{\hat{W}\}=0
\tag{45a}
$$

$$
[Q_W]\{\hat{W}\}+[Q_\Phi]\{\hat{\Phi}\}+[Q_\Theta]\{\hat{\Theta}\}+\frac{\gamma^2\cos^2\alpha}{12}\frac{g_2}{f_2}\lambda^2\{\hat{\Phi}\}=0
\tag{45b}
$$

$$
[P_W]\{\hat{W}\}+[R_\Phi]\{\hat{\Phi}\}+[R_\Theta]\{\hat{\Theta}\}+\frac{\gamma^2\cos^2\alpha}{12}\frac{g_2}{f_2}\lambda^2\{\hat{\Theta}\}=0
\tag{45c}
$$

where definition of matrices $[P_W]-[R_\Theta]$ are presented in Appendix A. Eqs. (45a)-(45c) can be written in the following compact form:

$$[K]\{U\} = \lambda^2 [M]\{U\} \tag{46}$$

In which

$$\{U\} = \begin{Bmatrix} \{\hat{W}\} \\ \{\hat{\Phi}\} \\ \{\hat{\Theta}\} \end{Bmatrix} \qquad [K] = \begin{bmatrix} [P_W] & [P_\Phi] & [P_\Theta] \\ [Q_W] & [Q_\Phi] & [Q_\Theta] \\ [R_W] & [R_\Phi] & [R_\Theta] \end{bmatrix}$$

$$[M] = -\frac{\gamma^2 \cos^2\alpha}{12} \begin{bmatrix} \dfrac{1}{kv_1}\dfrac{g_0}{f_0} I_{MN} & [0]_{MN} & [0]_{MN} \\ [0]_{MN} & \dfrac{g_2}{f_2} I_{MN} & [0]_{MN} \\ [0]_{MN} & [0]_{MN} & \dfrac{g_2}{f_2} I_{MN} \end{bmatrix} \tag{47}$$

It should be stated that in Eq. (47), $[0]_{MN}$ shows the zero matrix.

In a similar manner Eqs. (35a)-(35d) can be written using DQ rules as:

$$[T]\{U\} = \{0\} \tag{48}$$

where definition of matrix $[T]$ is presented in Appendix B.

In order to find eigen frequencies and corresponding eigen vectors, Eqs. (46) and (48) should be satisfied simultaneously. Let us divide the grid points as two sets: boundary points which are located at the four edges of the plate and domain ones which are other internal points. By neglecting of satisfying the Eq. (46) at the boundary points, this equation can be written as:

$$[\bar{K}]\{U\} = \lambda^2 [\bar{M}]\{U\} \tag{49}$$

where bar sign implies the corresponding non-square matrix. Eqs. (48) and (49) may be rearranged and partitioned in order to separate the boundary and domain points as the following:

$$[\bar{K}]_b \{U\}_b + [\bar{K}]_d \{U\}_d = \lambda^2 \left([\bar{M}]_b \{U\}_b + [\bar{M}]_d \{U\}_d \right) \tag{50a}$$

$$[T]_b \{U\}_b + [T]_d \{U\}_d = 0 \tag{50b}$$

where subscripts "b" and "d" indicate to the boundary and domain points, respectively. Substituting Eq. (50b) into Eq. (50a) leads to the following eigen value equation:

$$[F_K]\{U\}_d = \lambda^2 [F_M]\{U\}_d \tag{51}$$

In which

$$F_K = [\bar{K}]_d - [\bar{K}]_b [T]_b^{-1} [T]_d \qquad F_M = [\bar{M}]_d - [\bar{M}]_b [T]_b^{-1} [T]_d \tag{52}$$

5   NUMERICAL RESULTS AND DISCUSSION

Here the numerical results are given for the developed numerical solution in the previous section. First, in order to check the convergence of the proposed solution, consider a homogeneous skew plate($\mu_E = \mu_\rho = 1, \alpha = \beta = 15, \varphi = 1, \gamma = 0.1$ and $v = 0.3$); Fig. 3 shows effect of the number of grid points ($N = M$) on the value of the first six frequencies. As shown in this figure all frequencies converge for $N = M \rangle 11$.

To be sure of convergence in all of the following numerical examples, in what follows number of grid points are considered as $N = M = 15$. Also Poisson's ratio is considered as $v = 0.3$.

Consider a homogeneous skew plate ($\mu_E = \mu_\rho = 1, \alpha = \beta$); Table 1. shows the value of the six lowest dimensionless frequencies (λ) for various values of dimensionless width (φ), dimensionless thickness (γ) and skew angle (α). Comparing these results with those presented based on Ritz method [27], adaptation, accuracy and convergence of the proposed solution are confirmed. Also for $\varphi = 2, \gamma = 0.2, \alpha = 15$, the corresponding modes are depicted in Fig. 4.

Table 1
Values of the six lowest dimensionless frequencies (λ) of a homogeneous skew plate for various values of dimensionless width (φ), dimensionless thickness (γ) and skew angle (α).

| φ | γ | α | | Mode sequence number | | | | | |
				1	2	3	4	5	6
1	0.1	15	GDQM	3.523	8.472	20.98	24.97	30.70	47.40
			[27]	3.536	8.228	20.84	24.64	30.77	46.12
		30	GDQM	3.720	9.746	23.26	25.51	37.40	46.92
			[27]	3.858	8.870	23.23	24.27	37.03	45.24
	0.2	15	GDQM	3.420	7.746	18.17	22.05	25.97	38.73
			[27]	3.434	7.489	18.05	21.59	25.96	37.47
		30	GDQM	3.581	8.865	19.50	22.58	30.80	38.55
			[27]	3.719	8.055	19.51	21.34	30.57	37.00
2	0.1	15	GDQM	3.601	5.545	10.089	19.04	21.37	23.70
			[27]	3.594	5.366	9.949	18.28	21.42	23.24
		30	GDQM	3.994	6.027	10.21	18.49	24.92	29.14
			[27]	3.986	6.050	10.72	19.04	23.48	28.11
	0.2	15	GDQM	3.522	5.177	9.370	16.50	18.31	20.96
			[27]	3.493	5.071	9.178	16.43	18.47	20.80
		30	GDQM	3.818	5.901	9.987	17.03	20.26	24.53
			[27]	3.842	5.692	9.850	17.08	19.66	23.92

After validation of the proposed solution, the effect of the power law index, angles and thickness of the plate on the natural frequencies can be investigated. In what follows, results are given for a FG trapezoidal plate composed of Al / Al_2O_3 which its material properties are given in Table 2. [11].

Table 2
Material properties of the used FG plate [11].

| Material | Properties | |
	E (GPa)	ρ (Kg/m^3)
Aluminum (Al)	70	2702
Alumina (Al_2O_3)	380	3800

In order to clarify the behavior of Eqs. (1) and (2), Fig. 5(a) and 5(b) show the variation of the modulus of elasticity and density of the plate through the dimensionless thickness for various values of power law index (q); As shown in these figures, both modulus of elasticity and density decrease as value of the power law index grows.

Consider a FG plate with the following geometrical properties:

$$\varphi = 0.5 \qquad \gamma = 0.1 \qquad \alpha = 30° \qquad \beta = 15°$$

Table 3. shows the value of the six lowest dimensionless frequencies for various values of the power law index. As this table shows, all frequencies decrease as the value of the power law index increases. It reveals that the percentage of the decrease in modulus of elasticity is more than that in density. It should be noted that it is not a general conclusion and may change for the FG plates composed of other materials.

Table 3
Variation of the six lowest dimensionless frequencies of a trapezoidal plate for various value of power law index.

Mode sequence number	q (power law index)						
	0	0.2	0.5	1	1.5	3	5
1	8.068769	7.550972	7.088510	6.712589	6.528144	6.238277	5.967837
2	39.66892	37.16532	34.89616	33.00146	32.03556	30.48005	29.08282
3	63.92823	59.97921	56.32996	53.18332	51.51593	48.78840	46.43750
4	104.3074	97.90204	91.95563	86.77565	83.98494	79.34906	75.39665
5	156.9640	147.3776	138.4316	130.5818	126.3256	119.2611	113.2908
6	192.4295	180.9273	169.9932	160.0864	154.5024	145.0369	137.3002

A trapezoidal FG plate with the following properties is considered:

$$\varphi = 0.5 \qquad \gamma = 0.05 \qquad q = 2$$

The variation of the first six dimensionless frequencies versus that of angles of the plate ($\alpha \,\&\, \beta$) are depicted in Fig. 6. As depicted in this figure, the value of the frequencies increases as the value of α and β increase. Also for $\alpha = 15°$ and $\beta = 5°$ first six modes are depicted in Fig. 7.

According to Eqs. (19) and (34), the thickness of the plate is used in the definition of the dimensionless frequency (λ), before studying the effect of the thickness, let us define the following new dimensionless frequency:

$$\Omega^2 = \gamma^2 \lambda^2 = \frac{12(1-v^2)\rho_m b^2 \omega^2}{E_m}$$

which is independent of thickness. Now consider a trapezoidal plate with the following parameters:

$$\varphi = 0.5 \qquad \alpha = 15° \qquad \beta = 5° \qquad q = 1$$

Fig. 8 shows the effect of the dimensionless thickness on the six lowest dimensionless frequencies (Ω). It should be noted that in order to be able to show variation of all frequencies simultaneously, each frequency is divided to the corresponding value of a plate of($\gamma = 0.01(\Lambda_i = \Omega_i / \Omega_i^{\gamma=0.01}$). As shown, increasing in thickness increases all the frequencies. It happens because as the thickness of the plate grows, the plate rigidity will increase more than its translational and rotational inertias. It also can be concluded that value of the increase in frequencies diminishes at higher modes.
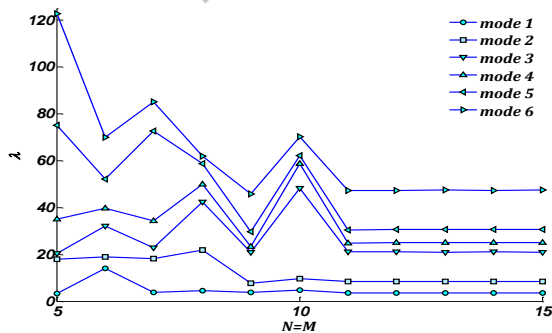

Fig.3
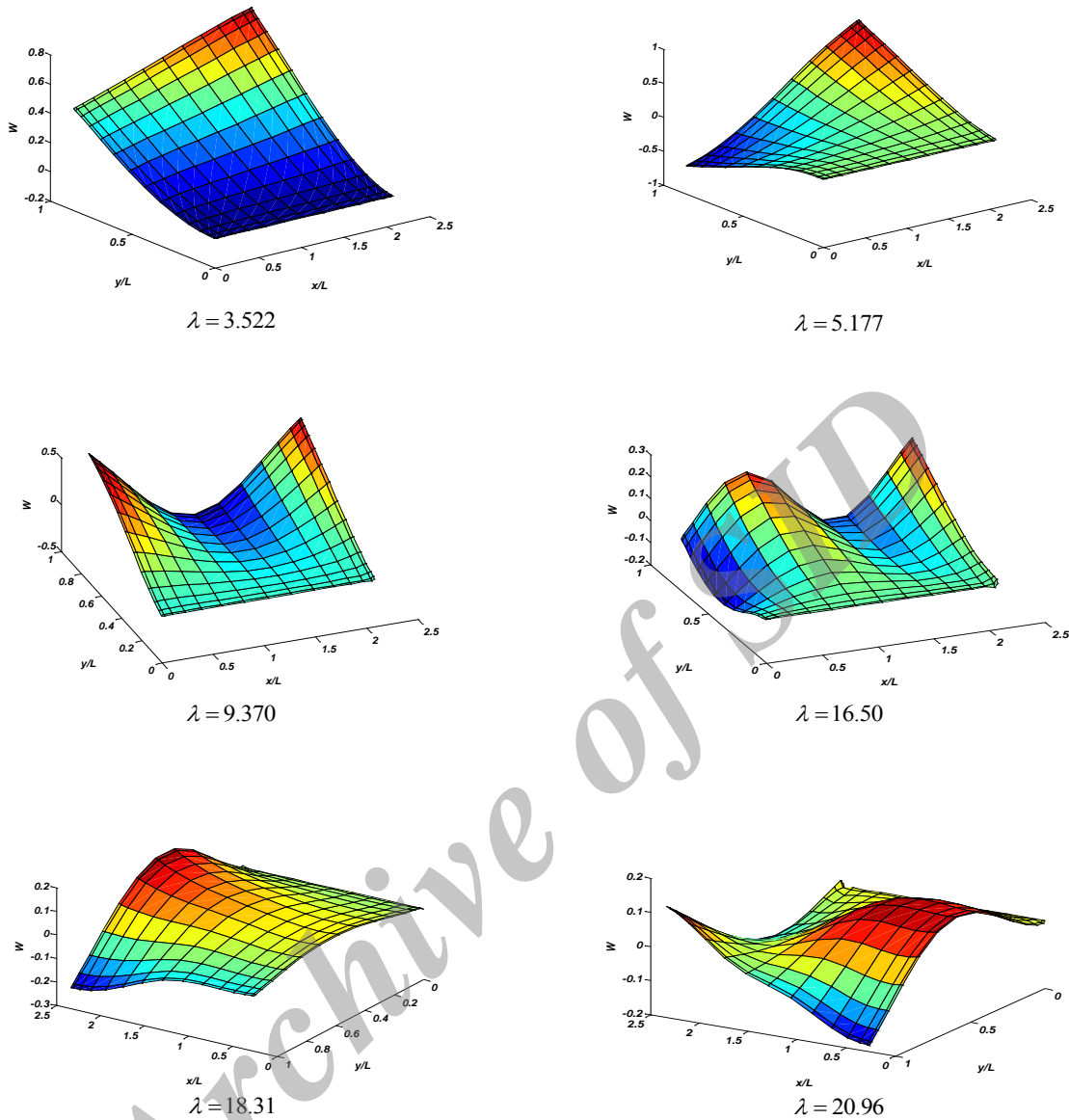Convergence of the first six frequencies of a skew plate.

$$\lambda = 3.522$$

$$\lambda = 5.177$$

$$\lambda = 9.370$$

$$\lambda = 16.50$$

$$\lambda = 18.31$$

$$\lambda = 20.96$$

Fig.4
Corresponding modes for six lowest frequencies of a skew plate of $\varphi = 2, \gamma = 0.2, \alpha = 15$.

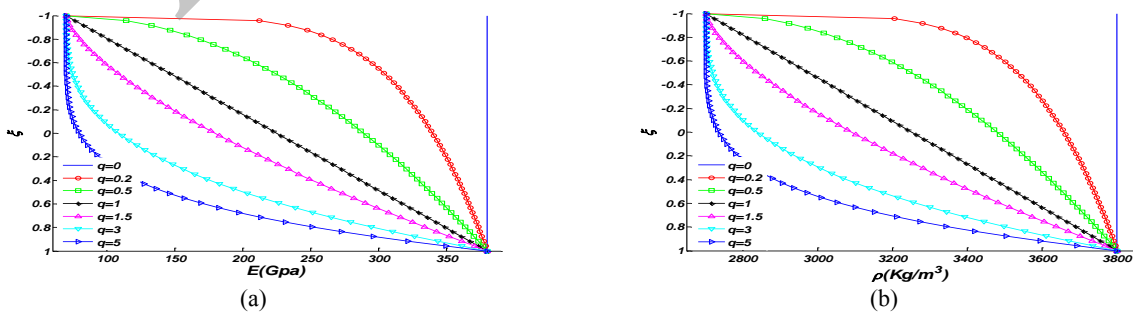(a)   (b)

Fig.5
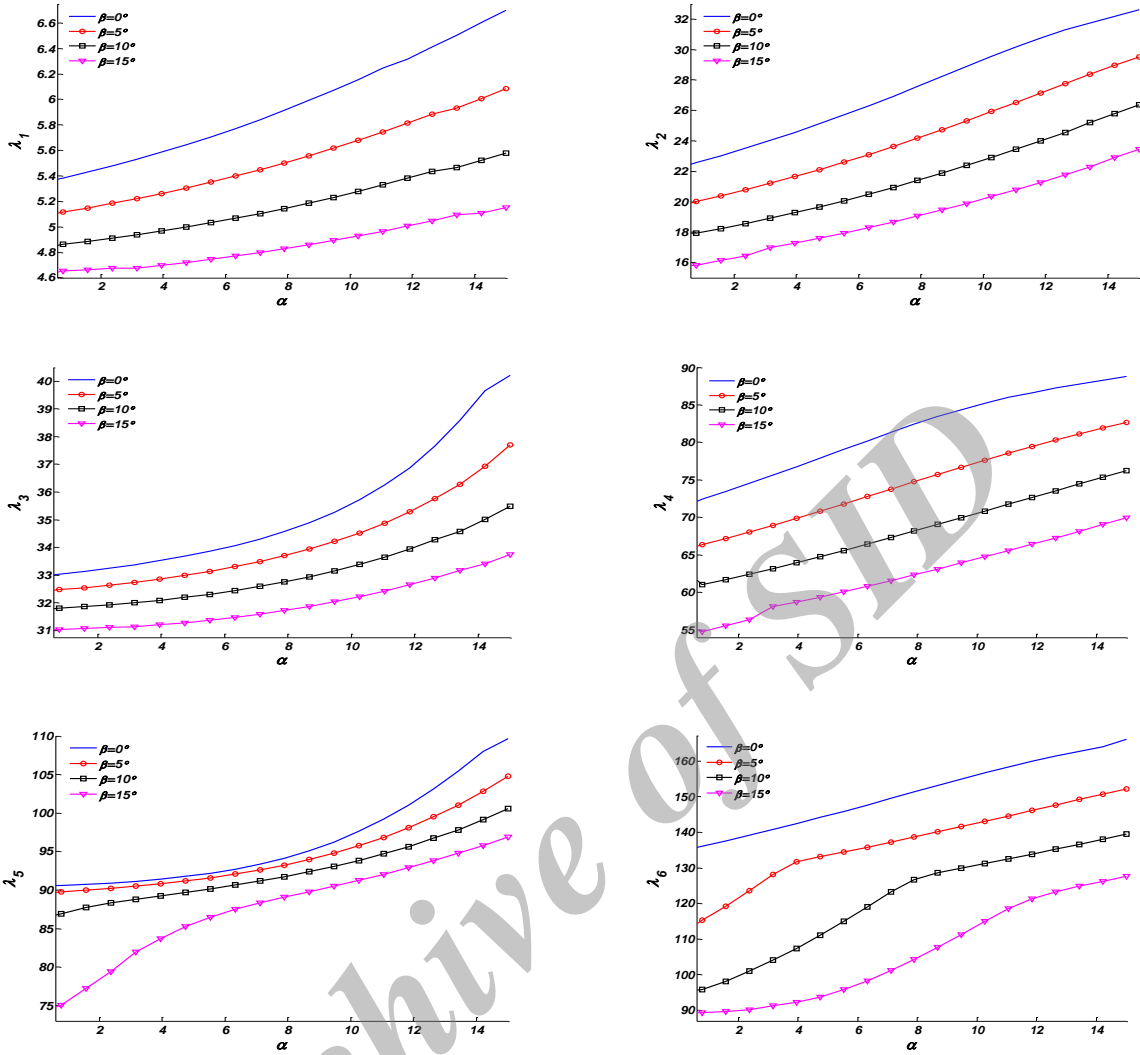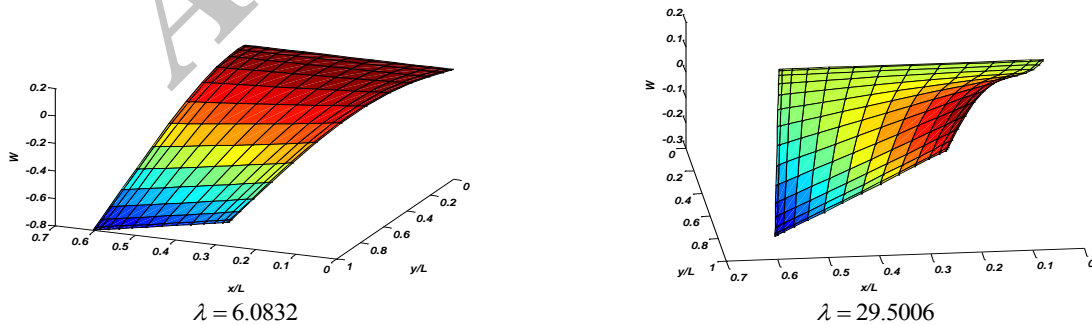Variation of Young's modulus and density through the dimensionless thickness of Al/Al_2O_3 plate.

Fig.6
Variation of the six lowest dimensionless frequencies versus variation of the angles of the plate ($\alpha \,\&\, \beta$).

$\lambda = 6.0832$

$\lambda = 29.5006$

$\lambda = 37.6949$

$\lambda = 82.6274$
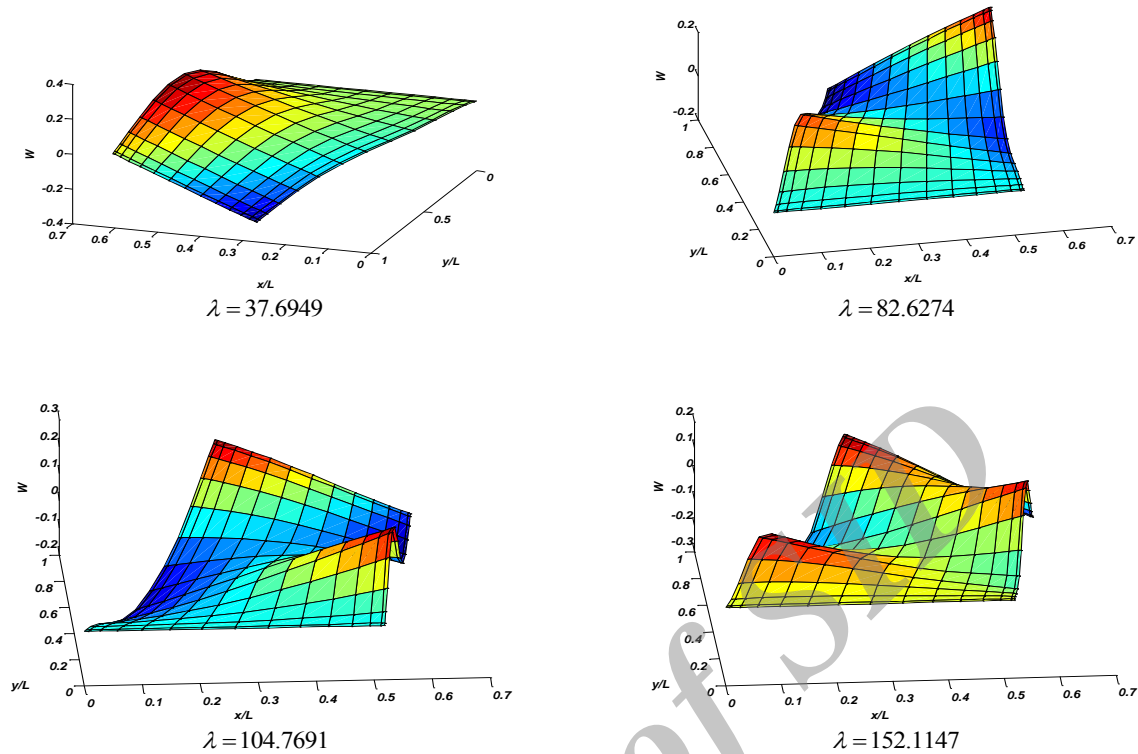
$\lambda = 104.7691$

$\lambda = 152.1147$

Fig.7

Corresponding modes for six lowest frequencies of a trapezoidal plate of $\alpha = 15^\circ$ and $\beta = 5^\circ$.
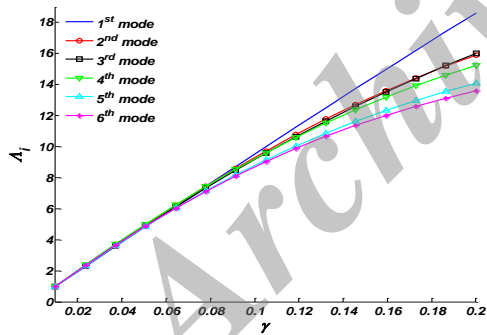

Fig.8
Variation of the six lowest dimensionless frequencies (Ω) versus dimensionless thickness of the plate.

6 CONCLUSIONS

Using Hamilton's principle and based on Reissner-Mindlin theory of plates, governing equations and boundary conditions for vibration analysis of a functionally graded thick plate was derived. In order to simplify the geometry of the problem, a transformation of coordinates was hired and governing equations and boundary conditions were rewritten in a new coordinate. Differential quadrature method was applied and natural frequencies and corresponding modes were derived numerically. Numerical results confirmed the accuracy and convergence of the method. Meanwhile, it was concluded that for a FG trapezoidal plate composed of Al/Al_2O_3, as the value of the power law index (q) grows, all frequencies decrease. Numerical examples also showed that as the value of the plate angles increase, all the frequencies grow. It is also concluded that all the frequencies grow with increasing the thickness of the plate.

APPENDIX A

Definition of matrices $[P_W]-[R_\Theta]$ appeared in Eqs. (45a)-(45c) are defined as follows:

$$
\begin{aligned}
[P_W] &= [e]^2 \otimes \left\{ \left(I_N + [f]^2\right)\left[B^{(\zeta)}\right] + 2G[f]\left[A^{(\zeta)}\right]\right\} + \left[B^{(\eta)}\right] \otimes I_N + 2[e]\left[A^{(\eta)}\right] \otimes [f]\left[A^{(\zeta)}\right] \\
[P_\Phi] &= \cos\alpha\,[e] \otimes \left[A^{(\zeta)}\right] \\
[P_\Theta] &= \cos\alpha \left\{\left[A^{(\eta)}\right] \otimes I_N + [e] \otimes [f]\left[A^{(\zeta)}\right]\right\} \\
[Q_W] &= -12 v_1 \frac{k\cos\alpha}{\gamma^2}\frac{f_0}{f_2}[e] \otimes \left[A^{(\zeta)}\right] \\
[Q_\Phi] &= [e]^2 \otimes \left\{\left[I_N + v_1[f]^2\right]\left[B^{(\zeta)}\right] + 2v_1 G[f]\left[A^{(\zeta)}\right]\right\} + v_1\left[B^{(\eta)}\right] \otimes I_N \\
&\quad + 2v_1[e]\left[A^{(\eta)}\right] \otimes [f]\left[A^{(\zeta)}\right] - 12 v_1 \frac{k\cos^2\alpha}{\gamma^2}\frac{f_0}{f_2} I_{MN} \\
[Q_\Theta] &= v_2 \left\{[e]\left[A^{(\eta)}\right] \otimes \left[A^{(\zeta)}\right] + [e]^2\left[B^{(\eta)}\right] \otimes [f] + G[e]^2 \otimes \left[A^{(\zeta)}\right]\right\} \\
[R_W] &= -12 v_1 \frac{k\cos\alpha}{\gamma^2}\frac{f_0}{f_2}\left\{\left[A^{(\eta)}\right] \otimes I_N + [e] \otimes [f]\left[A^{(\zeta)}\right]\right\} \\
[R_\Phi] &= v_2 \left\{[e]\left[A^{(\eta)}\right] \otimes \left[A^{(\zeta)}\right] + [e]^2 \otimes \left([f]\left[B^{(\zeta)}\right] + G\left[A^{(\zeta)}\right]\right)\right\} \\
[R_\Theta] &= \left[B^{(\eta)}\right] \otimes I_N + [e]^2 \otimes \left\{\left(v_1 I_N + [f]^2\right)\left[B^{(\zeta)}\right] + 2G[f]\left[A^{(\zeta)}\right]\right\} \\
&\quad + 2[e]\left[A^{(\eta)}\right] \otimes [f]\left[A^{(\zeta)}\right] - 12 v_1 \frac{k\cos^2\alpha}{\gamma^2}\frac{f_0}{f_2} I_{MN}
\end{aligned}
\tag{A.1}
$$

It should be noted that in Eq. $(A-1)$, $\otimes$ indicates the Kronecker product, I_N, I_M and I_{MN} are identity matrices and also $[e]$ and $[f]$ are diagonal matrices defined as:

$$
f_{ii} = F(\zeta_i) \qquad e_{jj} = E(\eta_j)
\tag{A.2}
$$

APPENDIX B

Definition of matrix $[T]$ appeared in Eq. (48) is considered as follows:

$$
[T] = \begin{bmatrix}
T_{11} & T_{12} & T_{13} \\
T_{21} & T_{22} & T_{23} \\
T_{31} & T_{32} & T_{33} \\
T_{41} & T_{42} & T_{43} \\
T_{51} & T_{52} & T_{53} \\
T_{61} & T_{62} & T_{63} \\
T_{71} & T_{72} & T_{73} \\
T_{81} & T_{82} & T_{83} \\
T_{91} & T_{92} & T_{93} \\
T_{101} & T_{102} & T_{103} \\
T_{111} & T_{112} & T_{113} \\
T_{121} & T_{122} & T_{123}
\end{bmatrix}
\tag{B.1}
$$

In which

$$\begin{aligned}
&\eta = 0 \qquad m = 1, 2, ..., M \\
&T_{11} = T_{22} = T_{33} = \delta_{1m} \otimes I_N \\
&T_{12} = T_{13} = T_{21} = T_{23} = T_{31} = T_{32} = \{0\}_{N*NM}
\end{aligned} \tag{B.2a}$$

$$\begin{aligned}
&\eta = 1 \qquad m = 1, 2, ..., M \\
&T_{41} = T_{51} = T_{62} = \{0\}_{N*NM} \\
&T_{63} = \{\delta_{Mm}\} \otimes I_N \\
&T_{42} = v T_{53} = \frac{v \cos\alpha \{\delta_{Mm}\} \otimes [A^{(\zeta)}]}{\varphi - G\cos\alpha} \\
&T_{43} = T_{52} = \{A_{Mm}^{(\eta)}\} \otimes I_N + \frac{\cos\alpha \{\delta_{Mm}\} \otimes [f][A^{(\zeta)}]}{\varphi - G\cos\alpha} \\
&T_{61} = \sec\alpha \{A_{Mm}^{(\eta)}\} \otimes I_N + \frac{\{\delta_{Mm}\} \otimes [f][A^{(\zeta)}]}{\varphi - G\cos\alpha}
\end{aligned} \tag{B.2b}$$

$$\begin{aligned}
&\eta = 0 \qquad n = 1, 2, ..., N \\
&T_{71} = T_{81} = \{0\}_{M*NM} \\
&-\tan\alpha\, T_{92} = T_{93} = \tan\alpha\, [I_M] \otimes \{\delta_{1i}\} \\
&T_{72} = (1 + \tan^2\alpha)[e] \otimes \{A_{1n}^{(\zeta)}\} - 2v_1 \tan\alpha [A^{(\eta)}] \otimes \{\delta_{1n}\} \\
&T_{73} = (v + \tan^2\alpha)\{A^{(\eta)}\} \otimes \{\delta_{1n}\} - \tan\alpha(1+\tan^2\alpha)[e] \otimes \{A_{1n}^{(\zeta)}\} \\
&T_{82} = (\tan 2\alpha - \tan\alpha)[e] \otimes \{A_{1n}^{(\zeta)}\} + [A^{(\eta)}] \otimes \{\delta_{1n}\} \\
&T_{83} = (1 + \tan\alpha - \tan 2\alpha)[e] \otimes \{A_{1n}^{(\zeta)}\} - \tan 2\alpha [A^{(\eta)}] \otimes \{\delta_{1n}\} \\
&T_{91} = \sec\alpha \tan\alpha \{A^{(\eta)}\} \otimes \{\delta_{1n}\} - \frac{1}{\cos^3\alpha}[e] \otimes \{A_{1n}^{(\zeta)}\}
\end{aligned} \tag{B.2c}$$

$$\begin{aligned}
&\zeta = 1 \qquad n = 1, 2, ..., N \\
&T_{101} = T_{111} = \{0\}_{M*NM} \\
&\tan\beta\, T_{122} = -T_{123} = \tan\beta\, [I_M] \otimes \{\delta_{1n}\} \\
&T_{102} = (1 + \tan^2\beta)[e] \otimes \{A_{Nn}^{(\zeta)}\} - 2v_1 \tan\beta [A^{(\eta)}] \otimes \{\delta_{Nn}\} \\
&T_{103} = (v + \tan^2\beta)\{A^{(\eta)}\} \otimes \{\delta_{Nn}\} - \tan\beta(1+\tan^2\beta)[e] \otimes \{A_{Nn}^{(\zeta)}\} \\
&T_{112} = (\tan 2\beta - \tan\beta)[e] \otimes \{A_{Nn}^{(\zeta)}\} + [A^{(\eta)}] \otimes \{\delta_{Nn}\} \\
&T_{113} = (1 + \tan\beta - \tan 2\beta)[e] \otimes \{A_{Nn}^{(\zeta)}\} - \tan 2\beta [A^{(\eta)}] \otimes \{\delta_{Nn}\} \\
&T_{121} = \sec\alpha(1 + \tan^2\beta)[e]\{A_{Nn}^{(\zeta)}\} - \sec\alpha \tan\beta \{A^{(\eta)}\} \otimes \{\delta_{Nn}\}
\end{aligned} \tag{B.2d}$$

It should be stated that in Eq. (B.2), δ is Kronecker delta defined as:

$$\delta_{ij} = \begin{cases} 1 & i = j \\ 0 & i \neq j \end{cases} \tag{B.3}$$

REFERENCES

[1]   Chopra I., Durvasula S., 1971, Vibration of simply supported trapezoidal plates I. symmetric trapezoids, *Journal of Sound and Vibration* **19**: 379-392.

[2]   Chopra I., Durvasula S., 1972, Vibration of simply supported trapezoidal plates II. un-symmetric trapezoids, *Journal of Sound and Vibration* **20**: 125-134.

[3]   Orris R.M., Petyt M., 1973, A finite element study of the vibration of trapezoidal plates, *Journal of Sound and Vibration* **27**: 325-344.

[4]   Srinivasan R.S., Babu B.J.C., 1983, Free vibration of cantilever quadrilal plates, *Journal of the Acoustical Society of America* **73**: 851-855.

[5]   Maruyama K., Ichinomiya O., Narita Y., 1983, Experimental study of the free vibration of clamped trapezoidal plates, *Journal of Sound and Vibration* **88**: 523-534.

[6]   Bert C.W., Malik M., 1996, Differential quadrature method for irregular domains and application to plate vibration, *International Journal of Mechanical Sciences* **38**: 589-606.

[7]   Xing Y., Liu B., 2009, High-accuracy differential quadrature finite element method and its application to free vibrations of thin plate with curvilinear domain, *International Journal for Numerical Methods in Engineering* **80**: 1718-1742.

[8]   Shufrin I., Rabinovitch O., Eisenberger M., 2010, A semi-analytical approach for the geometrically nonlinear analysis of trapezoidal plates, *International Journal of Mechanical Sciences* **52**: 1588-1596.

[9]   Zhou L., Zheng W.X., 2008, Vibration of skew plates by the MLS-Ritz method, *International Journal of Mechanical Sciences* **50**: 1133-1141.

[10]   Zamani M., Fallah A., Aghdam M.M., 2012, Free vibration analysis of moderately thick trapezoidal symmetrically laminated plates with various combinations of boundary conditions, *European Journal of Mechanics - A/Solids* **36**: 204-212.

[11]   Hosseini-Hashemi Sh., Fadaee M., Atashipour S.R., 2011, A new exact analytical approach for free vibration of Reissner–Mindlin functionally graded rectangular plates, *International Journal of Mechanical Sciences* **53**: 11-22.

[12]   Shaban M., Alipour M.M., 2011, Semi-analytical solution for free vibration of thick functionally graded plates rested on elastic foundation with elastically restrained edge, *Acta Mechanica Solida Sinica* **24**: 340-354.

[13]   Hasani Baferani A., Saidi A.R., Ehteshami H., 2011, Accurate solution for free vibration analysis of functionally graded thick rectangular plates resting on elastic foundation, *Composite Structure* **93**: 1842-1853.

[14]   Zhu P., Liew K.M., 2011, Free vibration analysis of moderately thick functionally graded plates by local Kriging meshless method, *Composite Structure* **93**: 2925-2944.

[15]   Hosseini-Hashemi Sh., Salehipour H., Atashipour S.R, Sburlati R., 2013, On the exact in-plane and out-of-plane free vibration analysis of thick functionally graded rectangular plates: Explicit 3-D elasticity solutions, *Composites Part B* **46**: 108-115.

[16]   Jin G., Su Z., Shi Sh., Ye T., Gao S., 2014, Three-dimensional exact solution for the free vibration of arbitrarily thick functionally graded rectangular plates with general boundary conditions, *Composite Structure* **108**: 565-577.

[17]   Xia P., Long S.Y., Cui H.X., Li G.Y., 2009, The static and free vibration analysis of a nonhomogeneous moderately thick plate using the meshless local radial point interpolation method, *Engineering Analysis with Boundary Elements* **33**: 770-777.

[18]   Huang M., Ma X.O., Sakiyama T., Matuda M., Morita C., 2005, Free vibration analysis of plates using least-square-based on finite difference method, *Journal of Sound and Vibration* **288**: 931-955.

[19]   Nguyen-Xuan H., Liu G.R., Thai-Hoang C., 2010, An edge-based smoothed finite element method (ES-FEM) with stabilized discrete shear gap technique for analysis of Reissner-Minslin, *Computer Methods in Applied Mechanics and Engineering* **199**: 471-489.

[20]   Leung A.Y.T., Zhu B., 2005, Transverse vibration of Mindlin Plates on two-parameter foundations by analytical trapezoidal p-elements, *Journal of Engineering Mechanics* **131**: 1140-1145.

[21]   Huang C.S., Leissa A.W., Chang M.J., 2005, Vibrations of skewed cantilevered triangular, trapezoidal and parallelogram Mindlin plates with considering corner stress singularities, *International Journal for Numerical Methods in Engineering* **62**: 1789-1806.

[22]   Abrate S., 2006, Free vibration, buckling, and static deflections of functionally graded plates, *Composites Science and Technology* **66**: 2383-2394.

[23]   Zhao X., Lee Y.Y., Liew K.M., 2009, Free vibration analysis of functionally graded plates using the element-free kp-Ritz method, *Journal of Sound and Vibration* **319**: 918- 939.

[24]   Eftekhari S.A., Jafari A.A., 2013, Modified mixed Ritz-DQ formulation for free vibration of thick rectangular and skew plates with general boundary conditions, *Applied Mathematical Modelling* **37**: 7398-7426.

[25]   Petrolito J., 2014, Vibration and stability analysis of thick orthotropic plates using hybrid-Trefftz elements, *Applied Mathematical Modelling* **38**:5858-5869.

[26]   Mindlin R.D., 1951, Influence of rotary inertia and shear on flexural motions of isotropic elastic plates, *Journal of Applied Mechanics* **18**: 31-38.

[27]   Liew K.M., Wang C.M., Xiang Y., Kitipornchai S., 1998, *Vibration of Mindlin Plates*, Elsevier.

[28]   Kaneko T., 1975, On Timoshenko's correction for shear in vibrating beams, *Journal of Physics D: Applied Physics* **8**: 1928-1937.

[29]   Bert C.W., Malik M., 1996, Differential quadrature method in computational mechanics: A review, *Applied Mechanics Reviews* **49**: 1-28.